

SCIENTIFIC REPORTS



OPEN

Mechanism of artemisinin resistance for malaria PfATP6 L263 mutations and discovering potential antimalarials: An integrated computational approach

Received: 20 January 2016

Accepted: 27 June 2016

Published: 29 July 2016

Nagasundaram N.¹, George Priya Doss C.², Chiranjib Chakraborty³, Karthick V.¹, Thirumal Kumar D.², Balaji V.⁴, Siva R.², Aiping Lu¹, Zhang Ge¹ & Hailong Zhu¹

Artemisinin resistance in *Plasmodium falciparum* threatens global efforts in the elimination or eradication of malaria. Several studies have associated mutations in the PfATP6 gene in conjunction with artemisinin resistance, but the underlying molecular mechanism of the resistance remains unexplored. Associated mutations act as a biomarker to measure the artemisinin efficacy. In the proposed work, we have analyzed the binding affinity and efficacy between PfATP6 and artemisinin in the presence of L263D, L263E and L263K mutations. Furthermore, we performed virtual screening to identify potential compounds to inhibit the PfATP6 mutant proteins. In this study, we observed that artemisinin binding affinity with PfATP6 gets affected by L263D, L263E and L263K mutations. This *in silico* elucidation of artemisinin resistance enhanced the identification of novel compounds (CID: 10595058 and 10625452) which showed good binding affinity and efficacy with L263D, L263E and L263K mutant proteins in molecular docking and molecular dynamics simulations studies. Owing to the high propensity of the parasite to drug resistance the need for new antimalarial drugs will persist until the malarial parasites are eventually eradicated. The two compounds identified in this study can be tested in *in vitro* and *in vivo* experiments as possible candidates for the designing of new potential antimalarial drugs.

The medicinal use of artemisinin (qinghaosu) from sweet wormwood (*Artemisia annua*) was explored in 1970 by Chinese scientist; since then it serves as a primary chemotherapy agent in antimalarial treatment. The number of malaria patients curing with artemisinin combined therapies has been increased exponentially¹ but the accurate molecular mechanism of action is still controversial². Artemisinin is a sesquiterpene lactone endoperoxide containing a structural feature called peroxide bridge and assumed to be crucial for the mode of action¹. Initial research suggests that the mechanism of action of artemisinin is by heme-dependent activation of an endoperoxide bridge occurring within the parasite's food vacuole^{3,4}. However, localization of artemisinin to the parasite and not food vacuole membranes⁵ and killing of tiny rings lacking haemozoin argue against the food vacuole being a major site of drug action⁶. Some other studies proposed a different mode of action of artemisinin, which is based on compound structural resemblance and the sesquiterpene moieties of thapsigargin. Thapsigargin is a plant product from *Thapsia garganica* shows structural similarities to artemisinin. Thapsigargin is considered as a highly selective inhibitor of Sarco/endoplasmic reticulum Ca²⁺-ATPase (SERCA). Based on this it was hypothesized that artemisinin may act in a similar way, but selectively to inhibit the SERCA of the malarial parasite. PfATP6 is the only SERCA-type Ca²⁺-ATPase enzyme present in the malarial parasite and it is considered to be

¹School of Chinese Medicine, Hong Kong Baptist University, Kowloon Tong, Hong Kong. ²School of Biosciences and Technology, VIT University, Vellore 632014, Tamil Nadu 632014, India. ³Department of Bioinformatics, School of Computer and Information Sciences, Galgotias University, Greater Noida, Uttar Pradesh, India. ⁴Department of Clinical Microbiology, Christian Medical College, Vellore 632014, Tamil Nadu, India. Correspondence and requests for materials should be addressed to Z.H. (email: hlzhu@hkbu.edu.hk)



Figure 1. Phylogenetic tree. Phylogenetic tree shows the evolutionary relationship between malarial PfATP6 protein and template (3TLM, 1IWO, and 2DQS) protein sequences.

the suitable molecular target for artemisinin⁵. An *in vitro* examination also suggests that artemisinin inhibit the SERCA-type Ca²⁺-ATPase orthologue (PfATP6) of *P. falciparum* in Xenopus oocytes⁷.

The successful progress of the elimination of malaria with artemisinin combination therapy is now hindered by the spreading antimalarial drug resistance. Artemisinin resistance is evident from slow parasite clearance^{8,9} and which affects the susceptibility of ring stage parasites^{10–14}. In western Cambodia first artemisinin resistance was reported^{8,9} followed by resistance rates for artemisinin based combination therapies were exponentially increasing¹⁵. Artemisinin resistance is also declared in mainland Southeast Asia; here it emerges independently and started to spread rapidly^{16–19}. Amino acid mutation at position 263 of PfATP6 enzyme tremendously affects the sensitivity of the enzyme to artemisinin and is located in the artemisinin binding pocket²⁰. *In vitro* studies in *X. laevis* oocytes elucidated that the substitution of a single amino acid residue L263A or L263S resulted in an approximately three-fold increase or decrease in sensitivity to artemisinin. Particularly the substitution of L263E leads to complete abolishment of interaction by artemisinin²⁰. However, this observation was not extended to *P. falciparum*, where introduction of the L263E mutation through transgenics resulted in borderline non-significant changes in the 50% inhibitory concentrations (IC50s) for artemisinin and its derivatives²¹. Recent report from Uhlemann *et al.* in 2012²⁰ stated the reconfirmation of their previous conclusion that single amino acid mutations in PfATP6 can abolish sensitivity to artemisinin, as shown by the results obtained with PfATP6 mutants L263D, L263E and L263K. These observations hypothesised that mutations in the particular residue L263 residing in drug binding pocket might affect the affinity of the drug and consecutively cause decreased susceptibility to artemisinin.

In the proposed study, we carried out molecular modeling of malaria PfATP6 protein and molecular docking between wild type PfATP6-Artemisinin and mutant type (L263D, L263E and L263K)-Artemisinin to elucidate the detailed mechanism of binding action. Further structure-based virtual screening was performed to identify novel lead molecules to inhibit the mutant PfATP6 proteins. To ensure the stability of protein-ligand complexes 50 ns united atom molecular dynamics simulation was performed thrice for the wild type and mutant type PfATP6-Artemisinin and mutant PfATP6-Virtually screened compounds.

Results

Homology modeling of malarial PfATP6 protein. The protein sequence of PfATP6 is composed of 1228 amino acids residues retrieved from the UniProt²² database. In BLAST sequence similarity analysis PfATP6 of *Plasmodium falciparum* obtained highest sequence homology (45% identity) with Endoplasmic Reticulum Ca²⁺-Atpase (SERCA) from the bovine muscle of Bos taurus. The tertiary structure of PfATP6 can be modelled by using the crystal structure of the SERCA homologue (PDB: 3TLM, resolution 2.95 Å)²³. Modelling of PfATP6 enzyme based on templates (1IWO and 2DQS) and docking of artemisinin derivative on to it was reported earlier by Jung *et al.* and Naik *et al.*^{24,25}. They observed good correlation between the computational binding affinity results and *in vitro* antimalarial sensitivity. Both 1IWO and 2DQS templates are from the same organism Oryctolagus cuniculus bound with thapsigargin but having closed conformation of calcium pump. In order to select the best template for 3D model construction phylogenetic tree analysis was performed between malarial PfATP6, 3TLM, 1IWO and 2DQS protein sequences. From the phylogenetic analysis result it is observed that malarial PfATP6 protein sequence and SERCA protein sequence from the bovine muscle of Bos taurus are evolutionarily more close (Fig. 1). Moreover, the binding affinity achieved by several docking and scoring methods could not differentiate between inhibitor and non-inhibitor in closed model of PfATP6. In this study, our ultimate goal is to seek a plausible mechanism action of artemisinin binding with wild and L263 mutant PfATP6 enzyme. Hence we studied from the model which is built using open conformation template (3TLM) of the enzyme to see the dynamic effect of protein-ligand complex along with the solvent. The sequences of PfATP6 and the bovine muscle of Bos taurus SERCA were aligned using ClustalW 2.0.1²⁶. The 3D structure of PfATP6 protein (Fig. 2) was constructed by using Modeller 9.15^{27,28}. The quality of the refined PfATP6 model was assessed by PRO-CHECK²⁹. The distribution of the Psi/Phi torsion angles of the best model is represented by a Ramachandran plot (Fig. 3), which shows 85.1% of residues are in most favored regions, 11.8% in additional allowed regions, 2.2% in generously allowed regions and 0.9% in disallowed regions. The calculated Ramachandran Z-score is 0.168, meaning that there is a good agreement between the PfATP6 model and the SERCA template.

Docking analysis of artemisinin with wild and mutant (L263D, L263E and L263K) malarial PfATP6 proteins. Artemisinin (Fig. 4) has been suggested to inhibit the *in vitro* activity of the malarial PfATP6 protein^{30,7}. Several studies have been attempted to find the binding mechanism of artemisinin with malarial PfATP6 protein^{23,24}. Additionally protein structure based drug design approaches have followed to optimise inhibitor binding specificity^{25,31}. In this study, we explored the appropriate binding conformation and affinity of artemisinin with wild and mutant PfATP6 proteins using a computational docking program Auto Dock Vina³². The PfATP6 protein's ligand binding residues were identified with thapsigargin as the reference ligand. The ligand binding site is close to the centre of the four transmembrane helices. Even minor conformational change in these

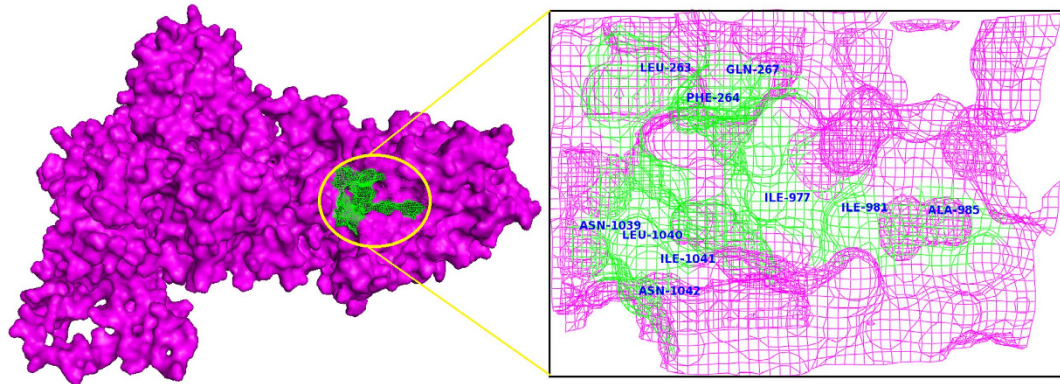


Figure 2. 3D structure of homology modeled malarial PfATP6 protein highlighted with artemisinin binding residues.

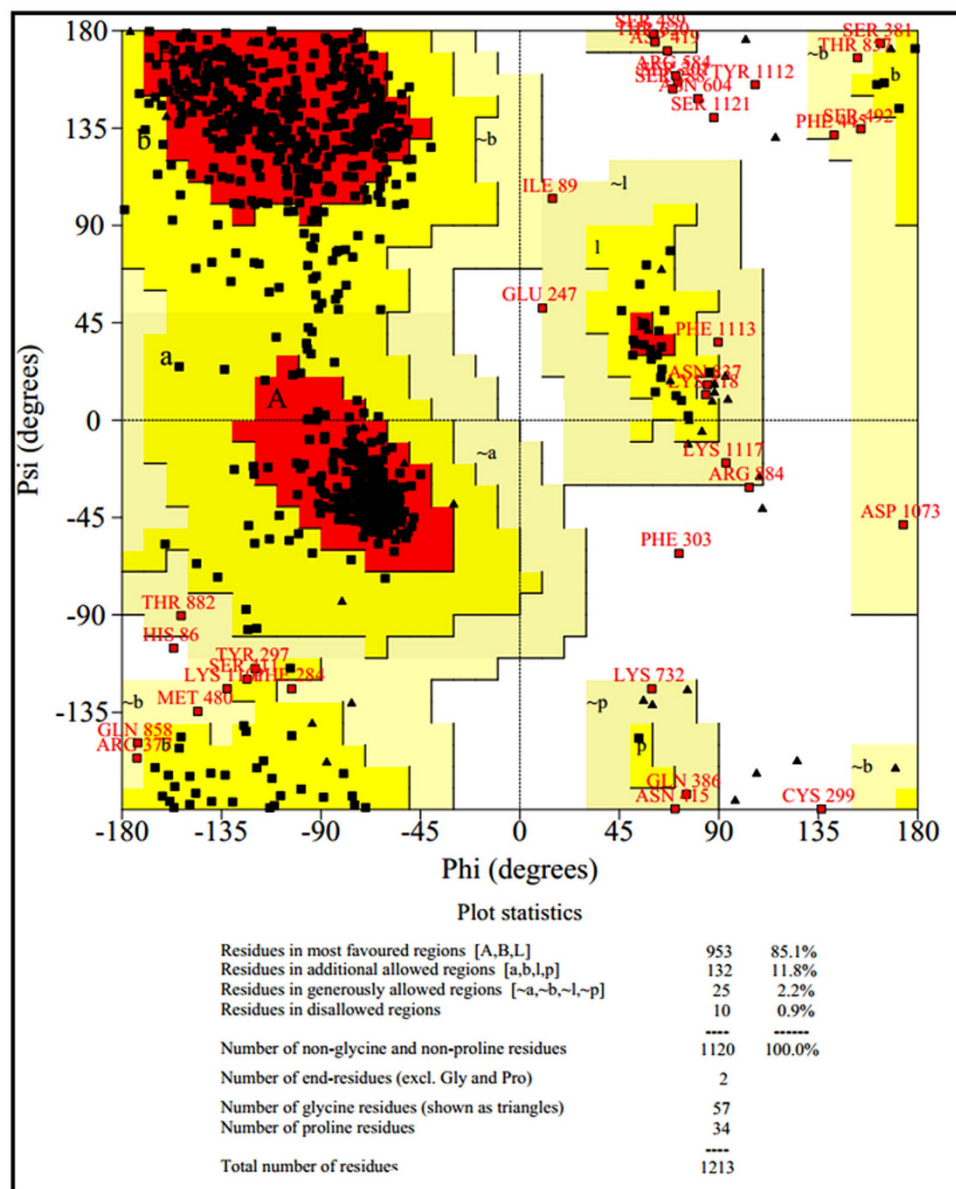
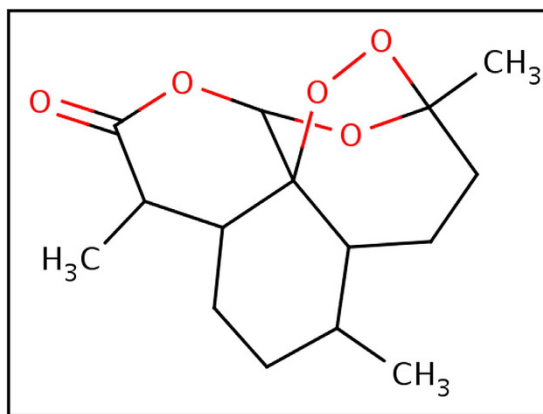
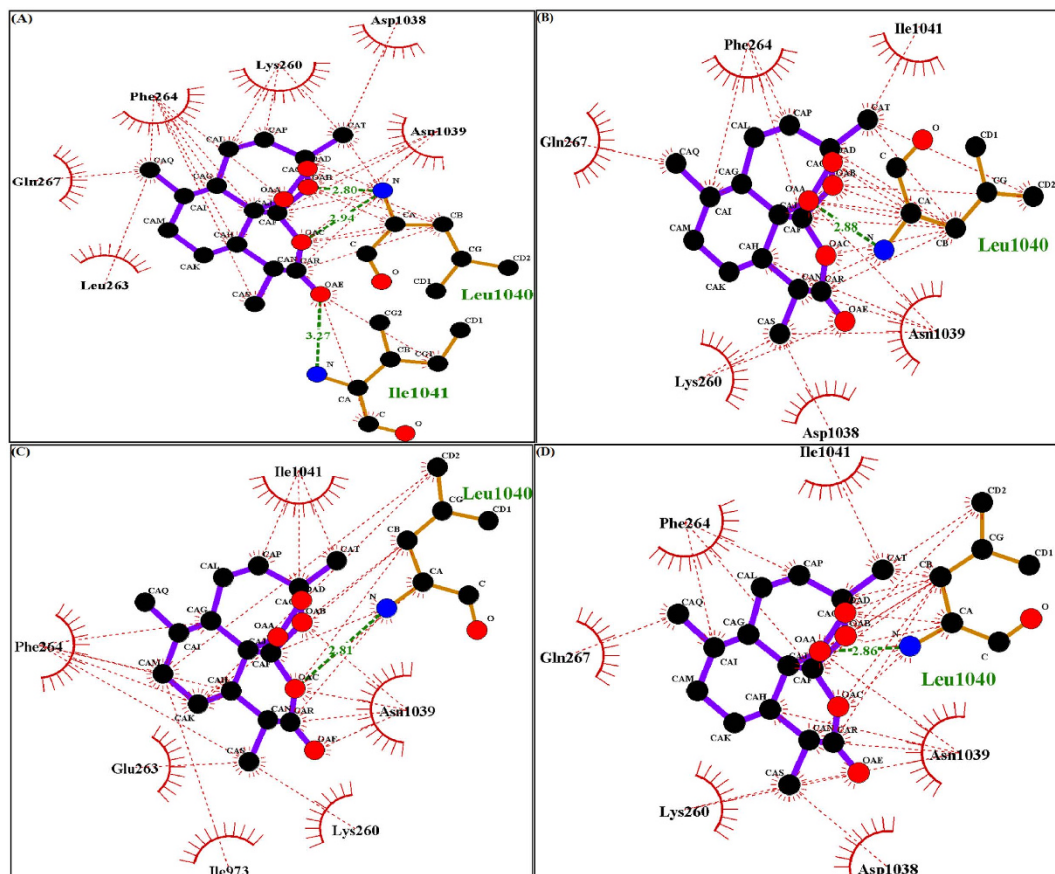


Figure 3. Ramachandran plot of a protein structure derived from homology modeling. It provides an overview of allowed and disallowed regions of torsion angle values, serving as an important indicator of the quality of protein three dimensional structures.

**Figure 4.** 2D image of drug artemisinin.**Figure 5.** Ligplot analysis of PfATP6 wild type-artemisinin and mutant types -artemisinin complexes, green lines indicates the hydrogen bonds and red dotted lines indicates the hydrophobic interactions. (A) Figure showing the wild type PfATP6 protein interacting residues with drug artemisinin. (B) Ligplot showing the interaction between mutant model L263D and artemisinin. (C) Ligplot showing the interaction between mutant typeL263E and artemisinin. (D) Ligplot showing the interaction between mutant typeL263K and artemisinin.

helices could affect the Ca²⁺ binding sites and thereby change the movement of ions to the luminal spaces or cytosol^{33–35}. The active site residues of PfATP6 consists of LEU263, PHE264, GLN267, ILE977, ILE981, ALA985, ASN1039, LEU1040, ILE1041, and ASN1042. In this computational docking analysis, artemisinin perfectly binds at the active site residues of PfATP6 enzyme (Fig. 5A) which are inconsistent with the results reported earlier^{24,31}. However, in the mutant PfATP6 proteins (L263D, L263E and L263K) artemisinin binds with different residues when compared to the wild type-artemisinin binding sites (Fig. 5B–D). The difference in the binding residues in mutant protein will indeed change the complementarities of artemisinin bindings with mutant PfATP6 proteins.

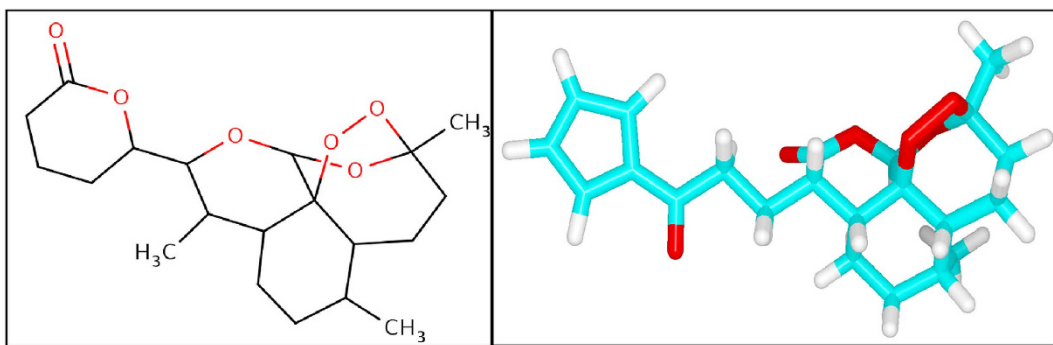


Figure 6. 2D and 3D image of compound CID 10595058.

Shape complementarity and non-covalent interactions are the crucial factors involved in the maintenance of protein-ligand stability. Van der Waals forces, hydrogen bonds, and electrostatic interactions are the primary non-covalent bonds that enhances the protein-ligand affinity. Calculating the non-covalent bond interaction energy is the important parameter in understanding the binding affinity between the protein-ligand molecules. Number of hydrogen bonds arises between the protein-ligand was calculated in Autodock vina. Artemisinin form three hydrogen bonds with wild type PfATP6 protein and one hydrogen bond with L263D, L263E, and L263K mutant protein structures. The binding energies between PfATP6 proteins and the inhibitor molecule artemisinin were calculated to be -8.4 kcal/mol , -7.2 kcal/mol , -7.4 kcal/mol and -7.1 kcal/mol for the wild type, L263D, L263E and L263K complexes respectively (Supplementary Table 1). The wild type-artemisinin complex obtained highest number of hydrogen bonds and binding energy, where as mutant complexes obtained less number of hydrogen bonds and binding energy. From this docking analysis it is concluded that these mutations L263D, L263E and L263K affected the binding affinity of artemisinin with PfATP6 protein and gives a theoretical assessment of the binding mechanism of PfATP6 wild and mutant proteins with antimalarial drug artemisinin.

PfATP6 mutant proteins structure-based virtual screening and docking studies. Different studies reported that single point mutations on PfATP6 of the malarial parasite were able to modulate the affinity of artemisinin for the protein and influencing efficacy and toxicity by affecting the artemisinin binding pocket^{7,20}. In this study also molecular docking analysis resulted that the PfATP6 mutations (L263D, L263E and L263K) affected the artemisinin binding affinity. The resistance of this malarial protein to the traditional artemisinin treatments has led to extensive work in discovering new drugs to treat malaria. *In silico*, virtual screening of chemical compounds is the fastest and most suitable method for identifying novel drug on the basis of target structures^{36,37}. Virtual screening of the existing compound have advantages over the *de novo* drug design approach because screened lead compounds can be immediately subjected to biological testing. Molecular docking is a robust method primary aim is to calculate binding affinities between a target protein and a ligand. Docking utilizes a defined search pattern to identify the most appropriate orientation of molecules and the binding score that describe the affinity of different conformations^{38,39}. For virtual screening, we retrieved 393 similar compounds like artemisinin from the PubChem database. Subsequently, docking analyses were performed between mutant PfATP6 proteins (L263D, L263E and L263K) and the screened compounds (Supplementary Table 2). Among the 393 compounds docked with the mutant structures, CID 10595058 binds with L263D and L263E and exhibits high binding affinity of -8.2 kcal/mol and -8.1 kcal/mol respectively (Fig. 6). This compound form three hydrogen bonds with L263D and L263E mutant protein structures (Fig. 7A,B). CID 10625452 (Fig. 8) binds with L263K mutant protein and exhibits high binding affinity -7.9 kcal/mol and forms two hydrogen bonds (Fig. 7C).

Analyzing molecular dynamics simulation studies. To verify the molecular docking binding affinity results robust or fortune molecular dynamics simulations analysis was performed for PfATP6-Artemisinin, L263D-Artemisinin, L263E- Artemisinin, L263K-Artemisinin, L263D-10595058, L263E-10595058, and L263K-10625452 protein-ligand complexes. The backbone RMSD informations for the wild and mutant type PfATP6-Artemisinin (Supplementary Fig. 1) and PfATP6-Virtually screened lead (Supplementary Fig. 2B) complexes were obtained from the respective trajectories. RMSD of second molecular dynamics run showed more stable convergence in comparison with other two runs was considered for further analysis. The backbone RMSD of wild type and mutant PfATP6-Artemisinin complexes attained stable equilibration after $\sim 10\text{ ns}$. But high fluctuations was observed for mutant PfATP6-Artemisinin complexes through out the simulation period and this reveals the existence of bad complementarity between mutant PfATP6 and artemisinin. For PfATP6-Virtually screened lead complexes immediate elevation in the RMSD was observed in the first $\sim 2000\text{ ps}$ due to the kinetic shock introduced during initial dynamic process. Later, the system maintained stable deviation pattern for the remaining simulation period. The overall energy was fluctuated around mean energy with the system equilibrating at one atmospheric pressure and at temperature of 310 K. The molecular dynamics simulation RMSD of the molecules attained stable after $\sim 20000\text{ ps}$ at the equilibrium. The PfATP6-Virtually screened lead complex trajectories attained stable RMSD values around $\sim 20000\text{ ps}$ indicating the stable binding affinity of the protein-ligand complexes. The initial and final structure of the protein-ligand complexes retrieved from the trajectories were shown in the Supplementary Figs 3 and 4.

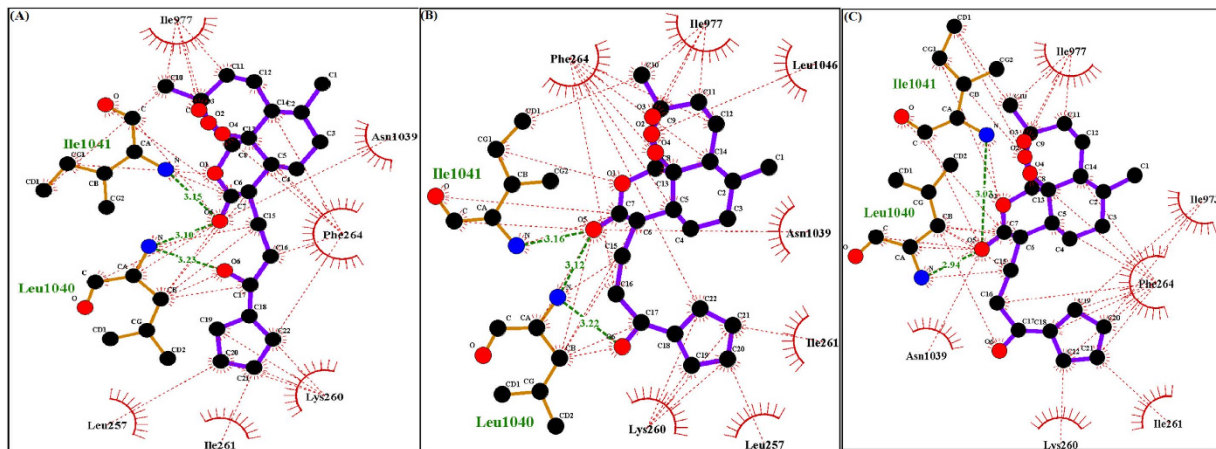


Figure 7. Ligplot analyses of PfATP6 mutant proteins with virtual compounds, green lines indicate the hydrogen bonds and red dotted lines indicates the hydrophobic interactions. (A) Ligplot showing interaction between mutant modelL263D and CID 10595058. (B) Ligplot showing interaction between mutant modelL263E and CID 10595058. (C) Ligplot showing interaction between mutant modelL263K and CID 10625452.

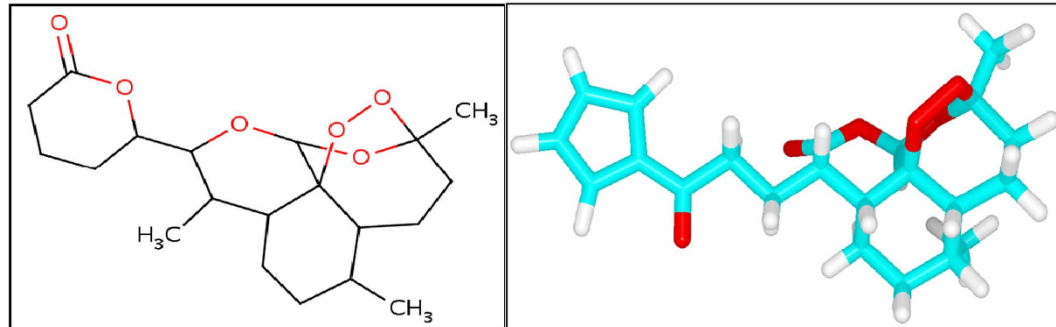


Figure 8. 2D and 3D image of compound CID 10625452.

Furthermore, to gain the knowledge on the contribution of micro-factors involvement in maintaining the binding affinity between protein-ligand complex, hydrogen bonds between molecules were analysed for wild type and mutant type PfATP6-Artemisinin and PfATP6-Virtually screened lead complexes in the simulation period of last 10 ns. The number of hydrogen bonds formed between wild type and mutant type PfATP6-Artemisinin (Supplementary Fig. 5) and PfATP6-Virtually screened compounds (Fig. 9) were analysed. Wild type PfATP6-Artemisinin obtained one to five hydrogen bonds in the last 10 ns simulation period. But the mutant type PfATP6 L263D, L263E and L263K obtained less number of hydrogen bonds 0 to 2, 0 to 2 and 0 to 3 respectively with anti-malarial drug artemisinin. This shows binding affinity of artemisinin drastically affected in the presence of L263 mutations at the binding pocket of target PfATP6 protein. The numbers of hydrogen bonds formed between L263D-10595058, L263E-10595058 and L263K-10625452 complexes were observed as 1 to 4, 1 to 4 and 1 to 3 respectively. The number of hydrogen bonds between the mutant proteins L263D, L263E and L263K with their respective virtually screened lead compounds is almost similar to the wild type PfATP6-Artemisinin complex. These results provided the evidence that the selected compounds have great calibre to function as strong inhibitors to the specific PfATP6 mutant protein.

The minimum distance between wild type and mutant type PfATP6-Artemisinin (Supplementary Fig. 6) and PfATP6-Virtually screened lead (Fig. 10) complexes were analyzed. The minimum distance between wild type PfATP6-Artemisinin is observed as ~1.5 to ~1.7 nm in the last 10 ns simulation period. But the minimum distance of mutants L263D, L263E and L263K with artemisinin were observed high as ~2.5 to ~2.7 nm, ~2.4 to ~2.6 nm, and ~2.4 to ~2.7 nm respectively. The minimum distance between L263D-10595058, L263E-10595058 and L263K-10625452 mutant proteins with virtually screened lead complexes is observed as ~2.1 to ~2.3 nm, ~2.4 to ~2.6 nm, and ~2.4 to ~2.6 nm respectively. The minimum distance between the mutant proteins and their respective lead compounds is much higher than the wild type PfATP6-Artemisinin complex. Even though the distances are slightly high but mutant PfATP6 proteins and virtually screened compounds are maintained stable contact and distance throughout the simulation period.

The area measured by the probe rolling on the surface of the protein is referred as the solvent-accessible surface area (SASA). This solvent effect is important in maintaining protein stability and act as a driving force for protein folding to be found in the burial of hydrophobic region. Likewise, this charged effect accompanies

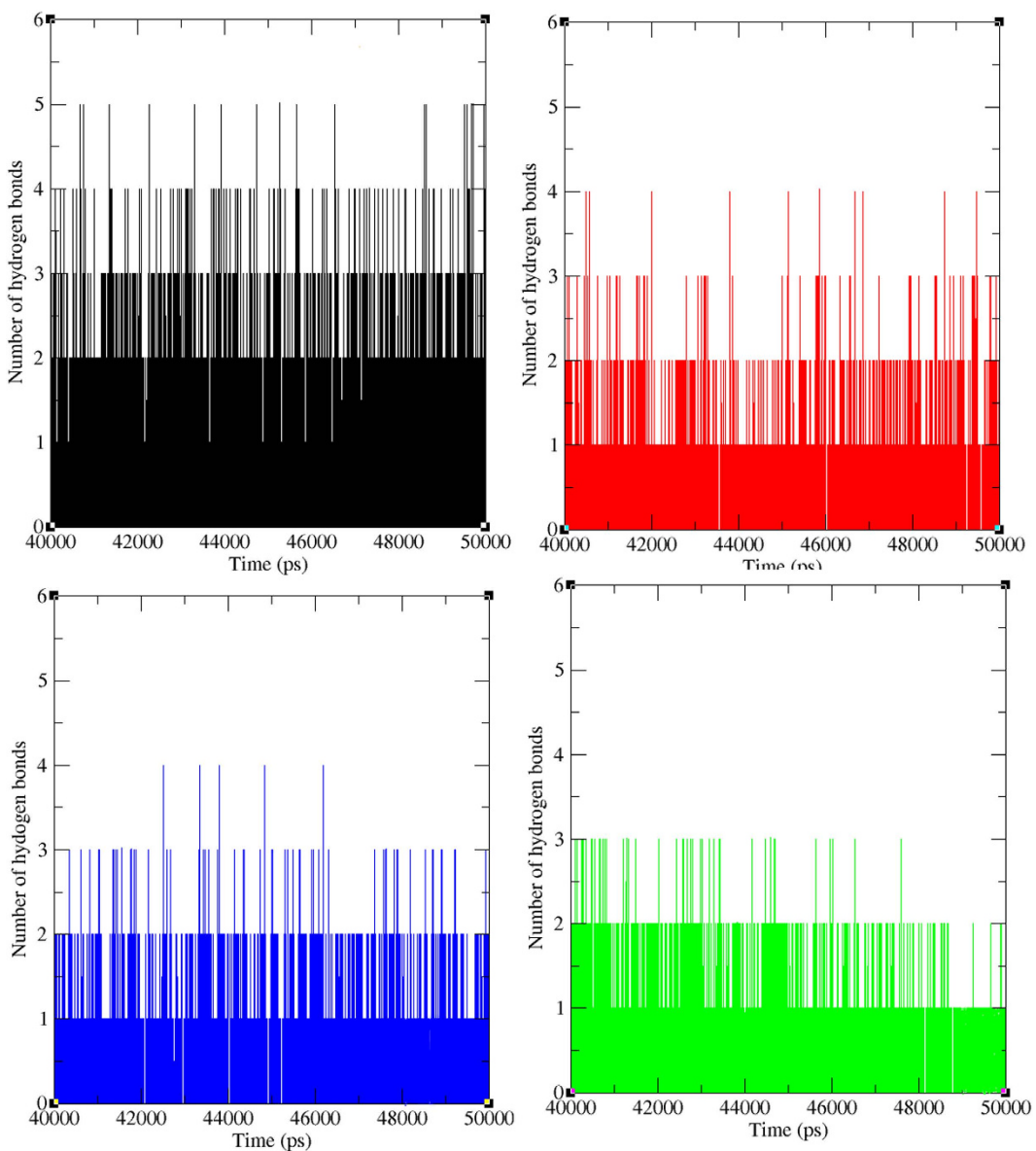


Figure 9. Total number of hydrogen bonds formed between protein-ligand in wild and mutant state. Black, Red, Green and Blue lines indicate the hydrogen bonds formed between wild type-artemisinin, L263D-10595058, L263E-10595058 and L263K-10625452 respectively.

protein-ligand interaction processes and reason for protein orientation maintenance. In molecular dynamic simulations, this accessible surface area of molecules are measured by using a sphere of water molecules⁴⁰. SASA was calculated for both the wild type and mutant PfATP6 proteins. From Fig. 11, it was observed that the wild-type PfATP6 have SASA of $\sim 133\text{ nm}^2$ to $\sim 147\text{ nm}^2$ in the last 10 ns simulation period but the mutant complexes L263D, L263E and L263K obtained less SASA of $\sim 130\text{ nm}^2$ to $\sim 142\text{ nm}^2$, $\sim 132\text{ nm}^2$ to $\sim 145\text{ nm}^2$, and $\sim 127\text{ nm}^2$ to $\sim 138\text{ nm}^2$ respectively. Compared with the wild type, all three mutated proteins obtained less SASA. This indicates that there might be orientational change in the protein surface because of the amino acid residue shift from the accessible area to buried region.

Discussion

Owing to the emerging resistance to existing antimalarial drugs there is a need for discovering novel drugs to treat malaria. Medicines for malaria venture and other product development partnerships initiated various drug discovery programs that reach milestone development of potential new antimalarial lead molecules^{41,42}, which are currently under clinical trials. Despite these successes, it is important to maintain early phase drug discovery to prevent the antimalarial drug development pipeline from draining^{43,44}. Rational post genomic drug discovery is based on the protein structure based screening of compounds from large chemical libraries either by high throughput or virtual screening methods. The primary focus of protein structure based drug design approach is the identification of a suitable drug. The target structure must essential for the survival of the parasite and

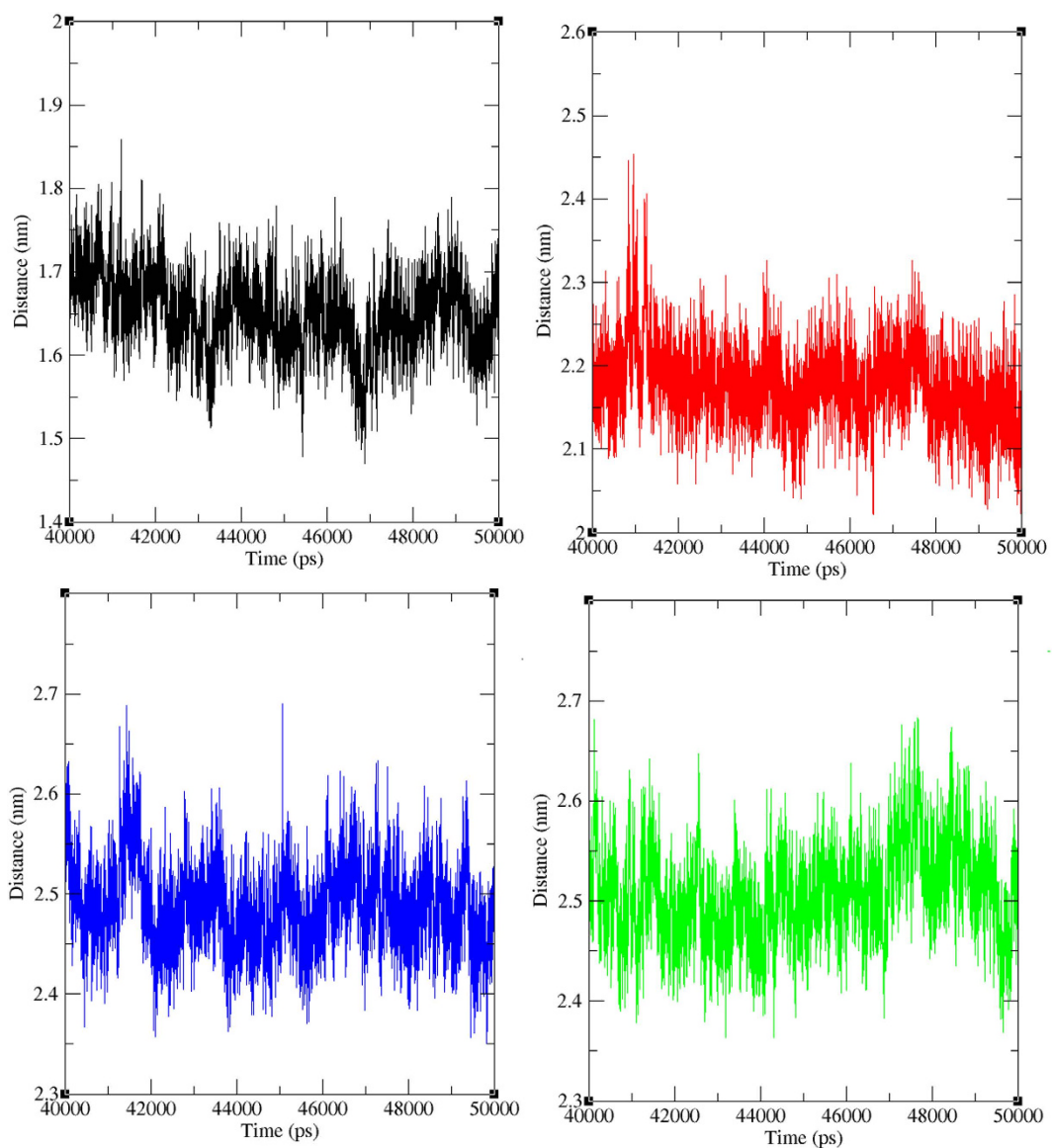


Figure 10. Minimum distance between protein-ligand in wild and mutant state. Black, Red, Green and Blue lines indicate the minimum distance between wild type-artemisinin, L263D-10595058, L263E-10595058 and L263K-10625452 respectively.

sufficiently different from the similar family of proteins in the host species to be inhibited specifically/selectively. The emergence of resistance first-line antimalarial treatment drug artemisinin has recently begun to affect the processing of patients suffering from *P. falciparum* infections in western Cambodia^{8,9}. If the artemisinin resistance spreads, large population will be affected in public health, as there is no suitable drug to treat *P. falciparum*. Therefore, there is an immediate requirement in understanding the mechanisms of action of artemisinin because this information may contribute to set a pipeline for monitoring emerging resistance and further for the development of new antimalarial drugs⁴⁵.

Protein 3D modeling and molecular docking simulations studies of the PfATP6 sequence suggested that artemisinin might interact directly with malarial PfATP6^{21,29,30}. So far, few genes have been proposed to be associated with reduced sensitivities to artemisinin, but till now none of the hypothesis has been proved⁴⁶. Even though several studies have been conducted to elucidate the mechanism of artemisinin binding but the predicted mechanism of action is not completely understood, since PfATP6 molecular biology is the lack of phylogenetically close 3D structures that could serve as template.

In this study, we followed a systematic computational approach to explore the mechanism of binding action of artemisinin with PfATP6 protein and also elucidated the molecular basis of the artemisinin resistance to L263 mutations. Since the target PfATP6 protein structure yet not resolved, PfATP6 3D structure constructed through homology modelling by using 3TLM as a template structure. But in previous studies 1IWO and 2DQS protein's 3D structure were used as a template for the 3D structural construction for malarial PfATP6 protein. Sequence similarity and phylogenetic comparison between malarial PfATP6, 3TLM, 1IWO and 2DQS protein sequences

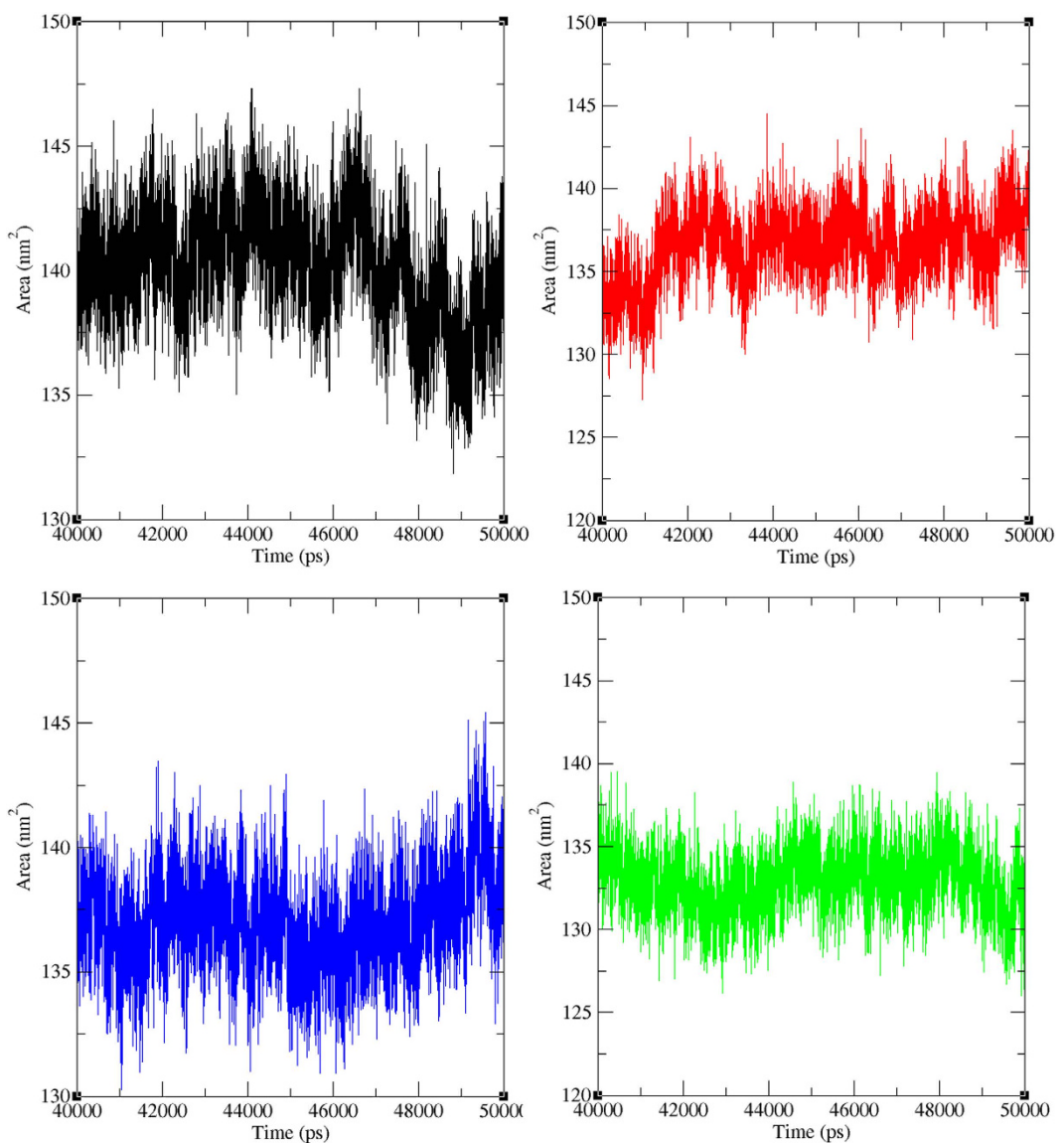


Figure 11. Solvent accessible surface area (SASA) analysis of wild and mutant PfATP6 proteins. Black, Red, Green and Blue lines indicate wild type, L263D, L263E, and L263K PfATP6 proteins respectively.

revealed that malaria PfATP6 and 3TLM protein sequence are evolutionarily closest. Our ultimate goal of this study is to elucidate the mechanistic action of artemisinin binding with wild and L263 mutant PfATP6 enzyme in open conformation model. Hence in this study 3TLM structure was used as the template to construct malarial PfATP6 3D structure. For structural analysis, we modelled the mutant (L263D, L263E and L263K) structures by using spdbv software. Following that, energy minimization was performed for the wild type and mutant PfATP6 proteins using steepest descent force field to maintain the geometry of the modelled protein. Next, docking analyses were performed between the wild type and mutant PfATP6 protein with drug artemisinin. Important factors maintaining the protein-ligand affinity were analysed. Binding energy between the mutant protein and drug revealed less binding affinity for the mutant structures with antimalarial drug artemisinin. Notably, artemisinin interacting residues differ in the mutant proteins and formed less number of hydrogen bonds than the wild type PfATP6 protein. These results confirmed that structural changes occurred in the PfATP6 protein because of L263 mutations. To identify a suitable inhibitor, structure-based virtual screening and docking analysis was performed. A total of 393 compounds that are structurally similar to antimalarial drug artemisinin were retrieved from the PubChem database. Each compound was individually docked with L263D, L263E and L263K mutant structures of malarial PfATP6 protein. CID 10595058 binds with L263D and L263E and this compound forms three hydrogen bonds with each of the mutant structure. CID 10625452 binds with L263K and forms two hydrogen bonds with L263K mutant structure.

Furthermore, we performed 50 ns MD simulation analysis on the wild type and mutant type PfATP6-Artemisinin and PfATP6-Virtually screened lead complexes. MD simulation analysis provides insights into the protein-ligand binding affinity and interactions at the atomic scale. Basic parameters RMSD, hydrogen

bond formation, minimum distance and SASA were examined on last 10 ns of protein-ligand simulation trajectories for PfATP6-Artemisinin, L263D-Artemisinin, L263E-Artemisinin, L263K-Artemisinin, L263D-10595058, L263E-10595058 and L263K-10625452 complexes. In the molecular stability change analysis all the mutant PfATP6-Artemisinin and mutant PfATP6-Virtually screened lead complexes obtained higher RMSD values than the wild type PfATP6-Artemisinin complex. Hydrogen bond formation between the protein and ligand served as the main contributor in maintaining the affinity and stability of the molecules. The substitution of amino acid changed the electrostatic potential in PfATP6 protein surface and affected the artemisinin binding. However, the virtually selected lead compound obtained strong binding affinity towards the mutant proteins and having the capability to maintain a stable number of hydrogen bonds during the simulation period. In all three mutant complexes (L263D-10595058, L263E-10595058, and L263K-10625452) almost same number of hydrogen bonds was observed as similar to wild type-artemisinin complex. The minimum distance formed between mutated proteins and the virtually screened potential lead compounds were slightly higher than the wild type PfATP6-artemisinin complex. Eventhough the distance is higher but it would not affect the affinity between molecules since the observed distance falls under the cut-off radii of non-bonded bonds formation limits. In SASA analysis, less solvent accessible surface were observed in all three mutant proteins in compare with wild type PfATP6 protein. Less accessible areas in mutant proteins might affect the probability of interactions between PfATP6 and artemisinin. Subsequently SASA results revealed that the occurrence of mutations in the PfATP6 protein changed the hydrophilic and hydrophobic areas of the mutant PfATP6 proteins and affected the artemisinin binding.

Conclusion

Despite increased support for malaria control over the past decade, the malaria burden remains high in many endemic countries. Prompt treatment with artemisinin based combination therapy targeted towards those confirmed to have malaria is a key malarial control strategy. Although artemisinin is a primary and quickly responding antimalarial drug, the curative rate of patients treated with *P. falciparum* malaria is decreased because of the emerging drug resistance. Due to the high propensity of the parasite to become drug resistant the need for new antimalarial drugs will persist until the malarial parasites are eventually eradicated. Because of several factors, the three-dimensional structure of plasmoidal proteins is not yet resolved through the physical approach. However, recent advancement in the computational techniques will helpful partially to overcome the traditional approach difficulties. This study is such one which describes the three-dimensional structure of malarial PfATP6 protein and then different *in silico* strategies were used to evaluate the resistant mechanism with artemisinin and well as subsequent rational approaches for identifying new lead molecules. The two compounds identified in this study can be tested *in vitro* and *in vivo* experiments as possible candidates for the designing of potential antimalarial medicines.

Materials and Methods

Protein homology modeling and refinement. The PfATP6 enzyme sequence of *P. falciparum* was obtained from UniProt²² database. The BLAST server⁴⁷ was used to search the closest sequence of PfATP6 in the RCSB Protein Data Bank. The high proportion of amino acid sequence identity between the target PfATP6 and endoplasmic reticulum Ca²⁺-ATPase (Serca) from bovine muscle (45% homology) indicates that crystal structure of the latter are good models, can be used as templates. The SERCA 3D structure of bovine muscle was obtained from the RCSB Protein Data Bank (PDB: 3TLM)²³. The sequence alignment of PfATP6 with SERCA as a reference was performed using ClustalW 2.0.1 by applying the default parameters. Protein reconstruction was achieved with Modeller 9.15 on the entire PfATP6 sequence^{27,28}. The refinement was made with the loop model class. The quality of each Modeller refined model was evaluated with PROCHECK (version 3.5.4)²⁹. The final model was chosen from both the PROCHECK results and the Modeller energy score. Hydrogen atoms were added, and the PfATP6 structure was minimized using the Gromos96 43a1 force field^{48,49}.

Docking and virtual screening. AutoDock is the widely accepted molecular docking programs and requires a set of preparation steps for general screening⁵⁰. Included in this process are preparations of acceptable ligands and a receptor macromolecule, calculation of maps and creation of folders for each ligand. AutoDock Vina is the updated version of AutoDock program with improved molecular docking and virtual screening strategies and was approximately two orders of magnitude faster than AutoDock⁴³. Vina uses a gradient optimisation method in its local optimisation procedure. The calculation of the gradient effectively gives the optimisation algorithm a “sense of direction” from a single evaluation. By utilizing the multi threading, Vina can produce fastest calculationon docking analysis by taking advantage of multiple CPUs or CPU cores. The assessment of the speed and accuracy of Vina during the flexible re-docking of 190 protein-ligand complexes demonstrated that the AutoDock4 training set was processed almost two orders of magnitude faster and with a significant improvement in binding mode prediction accuracy. Furthermore, Vina can further reduce computational time by utilising multiple CPU cores. The tool, VcPpt was used for high throughput virtual screening of compounds, VcPpt is an independently developed software package for flexible protein-ligand docking by the Biochem Lab solution.

Molecular dynamic simulations protocol. Molecular dynamics simulations of wild-type and mutant protein-ligand complexes were performed using Gromacs 5.0 software⁵¹. The force field used for energy minimization was Gromos96 43a1^{48,49}. The structures were solvated using a simple point charge (SPC) water box with a dimension of 52.0 Å. At physiological pH all the protein-ligand complexes obtained negative charges and to neutralize the system counter ions (Na⁺) were added in to the simulation box. Then, all the atoms in the box were energy minimized by applying the steepest descent algorithm. Next to the energy minimization, furthermore three steps have been followed i.e heating the system, equilibrating the system and finally the production of trajectories. The NPT (constant number of particles, pressure, and temperature) ensemble and then the NVT

(constant number of particles, volume and temperature) ensemble was performed at 300 K for 50000 ps⁵². Finally, the production of MD simulation was performed for 50 ns at 300 K. The covalent bonds were constrained by the Linear Constraint Solver (LINCS) algorithm⁵³. The Particle Mesh Ewald (PME) method was used to calculate electrostatic interactions⁵⁴. The cut-off radii for Coulomb interactions and van der Waals were fixed at 10.0 Å and 14.0, respectively.

By utilizing GROMACS utilities the trajectories obtained from each simulations were completely analyzed⁵⁵. The utilities g_rms, g_hbond, g_mindist and g_sas were used to plot RMSD, the number of hydrogen bonds formed between molecules, the minimum distances between molecules and solvent-accessible surface area (SASA) of proteins respectively. The numbers of hydrogen bonds and the minimum distance formed between protein-ligand complexes were calculated to explain the stability of the complexes. SASA analysis was performed to identify the traceable area of a molecule and all graphs were generated using the XM grace tool⁵⁶.

References

1. Klayman, D. L. Qinghaosu (artemisinin): an antimalarial drug from China. *Science* **228**, 1049–1055 (1985).
2. Arrow, K. J., Panosian, C. B. & Geltband, H. *Saving Lives, Buying Time*. (National Academies Press), doi:10.17226/11017 (2004).
3. Jefford, C. W. Why artemisinin and certain synthetic peroxides are potent antimalarials. Implications for the mode of action. *Curr. Med. Chem.* **8**, 1803–1826 (2001).
4. Pandey, A. V., Tekwani, B. L., Singh, R. L. & Chauhan, V. S. Artemisinin, an endoperoxide antimalarial, disrupts the hemoglobin catabolism and heme detoxification systems in malarial parasite. *J. Biol. Chem.* **274**, 19383–19388 (1999).
5. Ellis, D. S. *et al.* The chemotherapy of rodent malaria, XXXIX. Ultrastructural changes following treatment with artemisinine of Plasmodium berghei infection in mice, with observations of the localization of [³H]-dihydroartemisinine in *P. falciparum* *in vitro*. *Ann. Trop. Med. Parasitol.* **79**, 367–374 (1985).
6. Ter Kuile, F., White, N. J., Holloway, P., Pasvol, G. & Krishna, S. Plasmodium falciparum: *in vitro* studies of the pharmacodynamic properties of drugs used for the treatment of severe malaria. *Exp. Parasitol.* **76**, 85–95 (1993).
7. Eckstein-Ludwig, U. *et al.* Artemisinins target the SERCA of Plasmodium falciparum. *Nature* **424**, 957–961 (2003).
8. Noedl, H. *et al.* Evidence of artemisinin-resistant malaria in western Cambodia. *N. Engl. J. Med.* **359**, 2619–2620 (2008).
9. Dondorp, A. M. *et al.* Artemisinin resistance in Plasmodium falciparum malaria. *N. Engl. J. Med.* **361**, 455–467 (2009).
10. Saralamba, S. *et al.* Intrahost modeling of artemisinin resistance in Plasmodium falciparum. *Proc. Natl. Acad. Sci. USA* **108**, 397–402 (2011).
11. Witkowski, B. *et al.* Reduced artemisinin susceptibility of Plasmodium falciparum ring stages in western Cambodia. *Antimicrob. Agents Chemother.* **57**, 914–923 (2013).
12. Mok, S. *et al.* Artemisinin resistance in Plasmodium falciparum is associated with an altered temporal pattern of transcription. *BMC Genomics* **12**, 391 (2011).
13. Witkowski, B. *et al.* Novel phenotypic assays for the detection of artemisinin-resistant Plasmodium falciparum malaria in Cambodia: *in-vitro* and *ex-vivo* drug-response studies. *Lancet. Infect. Dis.* **13**, 1043–1049 (2013).
14. Chotivanich, K. *et al.* Laboratory detection of artemisinin-resistant Plasmodium falciparum. *Antimicrob. Agents Chemother.* **58**, 3157–3161 (2014).
15. World Health Organization Global Malaria Programme. Status report on artemisinin resistance. WHO/HTM/GMP/20149, 2014. Geneva: The Organization (2014).
16. Phyoe, A. P. *et al.* Emergence of artemisinin-resistant malaria on the western border of Thailand: a longitudinal study. *Lancet (London, England)* **379**, 1960–1966 (2012).
17. Amaratunga, C. *et al.* Artemisinin-resistant Plasmodium falciparum in Pursat province, western Cambodia: a parasite clearance rate study. *Lancet. Infect. Dis.* **12**, 851–858 (2012).
18. Kyaw, M. P. *et al.* Reduced susceptibility of Plasmodium falciparum to artesunate in southern Myanmar. *PLoS One* **8**, e57689 (2013).
19. Hien, T. T. *et al.* In vivo susceptibility of Plasmodium falciparum to artesunate in Binh Phuoc Province, Vietnam. *Malar. J.* **11**, 355 (2012).
20. Uhlemann, A. C. *et al.* A single amino acid residue can determine the sensitivity of SERCAs to artemisinins. *Nat. Struct. Mol. Biol.* **12**, 628–629 (2005).
21. Valderramos, S. G. *et al.* Identification of a mutant PfCRT-mediated chloroquine tolerance phenotype in Plasmodium falciparum. *PLoS Pathog.* **6**, e1000887 (2010).
22. Yip, Y. L., Lachenal, N., Pillet, V. & Veuthey, A.-L. Retrieving mutation-specific information for human proteins in UniProt/Swiss-Prot Knowledgebase. *J. Bioinform. Comput. Biol.* **5**, 1215–1231 (2007).
23. Sacchetto, R. *et al.* Crystal structure of sarcoplasmic reticulum Ca²⁺-ATPase (SERCA) from bovine muscle. *J. Struct. Biol.* **178**, 38–44 (2012).
24. Jung, M., Kim, H., Nam, K. Y. & No, K. T. Three-dimensional structure of Plasmodium falciparum Ca²⁺-ATPase(PfATP6) and docking of artemisinin derivatives to PfATP6. *Bioorg. Med. Chem. Lett.* **15**, 2994–2997 (2005).
25. Naik, P. K. *et al.* The binding modes and binding affinities of artemisinin derivatives with Plasmodium falciparum Ca²⁺-ATPase (PfATP6). *J. Mol. Model.* **17**, 333–357 (2011).
26. Larkin, M. A. *et al.* Clustal W and Clustal X version 2.0. *Bioinformatics* **23**, 2947–2948 (2007).
27. Sali, A. & Blundell, T. L. Comparative protein modelling by satisfaction of spatial restraints. *J. Mol. Biol.* **234**, 779–815 (1993).
28. Fiser, A., Do, R. K. & Sali, A. Modeling of loops in protein structures. *Protein Sci.* **9**, 1753–1773 (2000).
29. Laskowski, R. A., MacArthur, M. W., Moss, D. S. & Thornton, J. M. PROCHECK: a program to check the stereochemical quality of protein structures. *J. Appl. Crystallogr.* **26**, 283–291 (1993).
30. Gardner, M. J. *et al.* Genome sequence of the human malaria parasite Plasmodium falciparum. *Nature* **419**, 498–511 (2002).
31. Garah, F. B. E., Stigliani, J.-L., Cosledan, F., Meunier, B. & Robert, A. Docking studies of structurally diverse antimalarial drugs targeting PfATP6: no correlation between *in silico* binding affinity and *in vitro* antimalarial activity. *ChemMedChem* **4**, 1469–1479 (2009).
32. Trott, O. & Olson, A. J. AutoDock Vina: improving the speed and accuracy of docking with a new scoring function, efficient optimization, and multithreading. *J. Comput. Chem.* **31**, 455–461 (2010).
33. Toyoshima, C., Nakasako, M., Nomura, H. & Ogawa, H. Crystal structure of the calcium pump of sarcoplasmic reticulum at 2.6 Å resolution. *Nature* **405**, 647–655 (2000).
34. Toyoshima, C. & Nomura, H. Structural changes in the calcium pump accompanying the dissociation of calcium. *Nature* **418**, 605–611 (2002).
35. Ogawa, H., Stokes, D. L., Sasabe, H. & Toyoshima, C. Structure of the Ca²⁺ pump of sarcoplasmic reticulum: a view along the lipid bilayer at 9-Å resolution. *Biophys. J.* **75**, 41–52 (1998).
36. Ripphausen, P., Nisius, B., Peitason, L. & Bajorath, J. Quo vadis, virtual screening? A comprehensive survey of prospective applications. *J. Med. Chem.* **53**, 8461–8467 (2010).
37. Clark, D. E. What has virtual screening ever done for drug discovery? *Expert Opin. Drug Discov.* **3**, 841–851 (2008).

38. Cheng, T., Li, Q., Zhou, Z., Wang, Y. & Bryant, S. H. Structure-based virtual screening for drug discovery: a problem-centric review. *AAPS J.* **14**, 133–141 (2012).
39. Meng, X. Y., Zhang, H. X., Mezei, M. & Cui, M. Molecular docking: a powerful approach for structure-based drug discovery. *Curr. Comput. Aided. Drug Des.* **7**, 146–157 (2011).
40. Gerlt, J. A., Kreevoy, M. M., Cleland, W. W. & Frey, P. A. Understanding enzymic catalysis: the importance of short, strong hydrogen bonds. *Chem. Biol.* **4**, 259–267 (1997).
41. Charman, S. A. *et al.* Synthetic ozonide drug candidate OZ439 offers new hope for a single-dose cure of uncomplicated malaria. *Proc. Natl. Acad. Sci. USA* **108**, 4400–4405 (2011).
42. Rottmann, M. *et al.* Spiroindolones, a potent compound class for the treatment of malaria. *Science* **329**, 1175–1180 (2010).
43. Müller, I. B. & Hyde, J. E. Antimalarial drugs: modes of action and mechanisms of parasite resistance. *Future Microbiol.* **5**, 1857–1873 (2010).
44. Sa, J. M., Chong, J. L. & Wellemes, T. E. Malaria drug resistance: new observations and developments. *Essays Biochem.* **51**, 137–160 (2011).
45. Haynes, R. K. *et al.* Artemisone a highly active antimalarial drug of the artemisinin class. *Angew. Chem. Int. Ed. Engl.* **45**, 2082–2088 (2006).
46. Ding, X. C., Beck, H. P. & Raso, G. Plasmodium sensitivity to artemisinins: magic bullets hit elusive targets. *Trends Parasitol.* **27**, 73–81 (2011).
47. Altschul, S. F. *et al.* Gapped BLAST and PSI-BLAST: a new generation of protein database search programs. *Nucleic Acids Res.* **25**, 3389–3402 (1997).
48. Gunsteren, W. F. van. *Biomolecular Simulation: The GROMOS96 Manual and User Guide*. (Biomos ; Zurich, (1996).
49. Oostenbrink, C., Villa, A., Mark, A. E. & van Gunsteren, W. F. A biomolecular force field based on the free enthalpy of hydration and solvation: the GROMOS force-field parameter sets 53A5 and 53A6. *J. Comput. Chem.* **25**, 1656–1676 (2004).
50. Morris, G. M. *et al.* AutoDock4 and AutoDockTools4: Automated docking with selective receptor flexibility. *J. Comput. Chem.* **30**, 2785–2791 (2009).
51. Hess, B., Kutzner, C., van der Spoel, D. & Lindahl, E. GROMACS 4: Algorithms for Highly Efficient, Load-Balanced, and Scalable Molecular Simulation. *J. Chem. Theory Comput.* **4**, 435–447 (2008).
52. Berendsen, H. J. C., Postma, J. P. M., van Gunsteren, W. F., DiNola, A. & Haak, J. R. Molecular dynamics with coupling to an external bath. *J. Chem. Phys.* **81**, 3684 (1984).
53. Hess, B., Bekker, H., Berendsen, H. J. C. & Fraaije, J. G. E. M. LINCS: A linear constraint solver for molecular simulations. *J. Comput. Chem.* **18**, 1463–1472 (1997).
54. Essmann, U. *et al.* A smooth particle mesh Ewald method. *J. Chem. Phys.* **103**, 8577 (1995).
55. Van Der Spoel, D. *et al.*. GROMACS: fast, flexible, and free. *J. Comput. Chem.* **26**, 1701–1718 (2005).
56. Turner, P. J. XMGRACE, Version 5.1.19. Central for costal and Land-Margin Research; Oregon Graduate Institute of Science and Technology, Beaverton, ORE, USA (2005).

Acknowledgements

This work was supported by the Research Grants Council of Hong Kong 212613 and Faculty Research Grant of Hong Kong Baptist University FRG/14-15/063 and FRG2/13-14/056. The authors take this opportunity to thank the management of VIT University, Galgotias University and CMCH Vellore for providing the facilities and encouragement to carry out this work.

Author Contributions

N.N., G.P.D.C., C.C., K.V. and T.K.D. were involved in design, acquisition of data, analysis and interpretation of the data. N.N., G.P.D.C., C.C., K.V., B.V., T.K.D. and S.R. were involved in interpretation of the data and drafting the manuscript. A.L., Z.G. and H.Z. supervised the entire study and was involved in design, acquisition of data, analysis and interpretation of the data and drafting the manuscript. The manuscript was reviewed and approved by all the authors G.P.D.C., C.C. and H.Z.

Additional Information

Supplementary information accompanies this paper at <http://www.nature.com/srep>

Competing financial interests: The authors declare no competing financial interests.

How to cite this article: N., N. *et al.* Mechanism of artemisinin resistance for malaria PfATP6 L263 mutations and discovering potential antimalarials: An integrated computational approach. *Sci. Rep.* **6**, 30106; doi: 10.1038/srep30106 (2016).



This work is licensed under a Creative Commons Attribution 4.0 International License. The images or other third party material in this article are included in the article's Creative Commons license, unless indicated otherwise in the credit line; if the material is not included under the Creative Commons license, users will need to obtain permission from the license holder to reproduce the material. To view a copy of this license, visit <http://creativecommons.org/licenses/by/4.0/>

© The Author(s) 2016